JOURNAL OF GEOPHYSICAL RESEARCH: SPACE PHYSICS, VOL. 118, 1–9, doi:10.1002/jgra.50488, 2013

On the UT and seasonal variations of the standard and SuperMAG auroral electrojet indices

Anand K. Singh,[1,2] R. Rawat,[1,3] and B. M. Pathan[1]

Received 4 December 2012; revised 29 July 2013; accepted 30 July 2013.

[1] The standard auroral electrojet (*AE*) indices are based on magnetic disturbance data from 10 to 12 northern auroral observatories. Recently, Newell and Gjerloev (2011a) computed equivalent SuperMAG electrojet (*SME*) indices using data from around 100 mid latitude to high latitude observatories in the Northern Hemisphere. The *SME* indices certainly have advantage over the *AE* indices in terms of number as well as temporal resolution of substorm onsets due to better latitudinal and longitudinal coverage. The UT and seasonal variations of geomagnetic activity have been extensively examined in the past. However, particularly for the *AE* indices, these variations have remained elusive due to sparse distribution of the *AE* observatories. In this study, we examine what effect the inclusion of large number of stations would make on the UT and seasonal variations of the auroral electrojets activities. For this purpose, data for years 1997–2009 have been considered when consistently many stations (> 70) were available for the computation of the *SME* indices. We demonstrate that the *SME* indices exhibit grossly similar UT and seasonal variations as observed in the *AE* indices. However, there are subtle differences which arise due to difference in number of stations. Our study suggests that most of the UT and seasonal variations of the *AE* indices, reported earlier, were mainly not due the sparse distribution of stations, but rather to the actual physical processes that control them.

Citation: Singh, A. K., R. Rawat, and B. M. Pathan (2013), On the UT and seasonal variations of the standard and SuperMAG auroral electrojet indices, *J. Geophys. Res. Space Physics*, *118*, doi:10.1002/jgra.50488.

1. Introduction

[2] Ever since the introduction of the auroral electrojet (*AE*) indices (*AU* and *AL*) by *Davis and Sugiura* [1966], the scientific community has widely relied on them for substorm studies [e.g., *Vassiliadis et al.*, 1995] and their various effects [e.g., *Kamide et al.*, 1998; *Zhou et al.*, 2011; *Singh et al.*, 2012a]. However, the suitability of the *AE* indices for substorm identification has been questioned by several authors due to the inclusion of a limited number of longitudinally distributed auroral latitude ($\sim$ 60°N – 70°N) observatories [e.g., *Kamide and Akasofu*, 1983; *Rostoker*, 1972]. On one hand, during quiet magnetospheric conditions, the auroral oval contracts poleward and substorms occurring under such conditions may not be observed by the *AE* indices [e.g., *Singh et al.*, 2012b, and references therein], whereas equatorward expansion of auroral oval during very disturbed conditions, on the other hand, results in underestimation of the substorm intensity by the *AE* indices [*Ahn et al.*, 2000; *Rostoker*, 1972].

[3] The *AE* indices exhibit prominent UT and seasonal variations. Earlier studies [e.g., *Russell and McPherron*, 1973; *Basu*, 1975; *Berthelier*, 1976] suggested that the diurnal and seasonal changes in the effective interplanetary magnetic field contribute to the UT and seasonal variations of the geomagnetic activity. *Cliver et al.* [2000] reported that the angle between solar wind flow direction and Earth's dipole axis contributes to the UT and seasonal variations. As the global distribution of the standard *AE* stations is not uniform, *Ahn et al.* [2000] suggested that the combined effects of large longitudinal gaps between the *AE* stations and the equatorward expansion of the auroral electrojets play vital role for the UT variations. Moreover, changing ionospheric conductivity with seasons also introduces UT variation of the *AE* indices [*Ahn et al.*, 2000]. *Lyatsky et al.* [2001] studied the *AU* and *AL* indices separately and demonstrated that the solar illumination of the high-latitude ionosphere has important implications for the UT variations of geomagnetic activity.

[4] Owing to the limitations of the standard *AE* indices, particularly arising due to sparse latitudinal distribution of observatories, various local equivalent indices have been introduced using data from different networks of closely spaced high-latitude observatories. For example, *IE* indices from the International Monitor for Auroral

[1]Indian Institute of Geomagnetism, Navi Mumbai, India.
[2]Now at ESSO-National Centre for Antarctic and Ocean Research, Vasco da Gama, India.
[3]Now at Instituto Nacional de Pesquisas Espaciais, Sao Jose dos Campos, Sao Paulo, Brazil.

Corresponding author: A. K. Singh, ESSO-National Centre for Antarctic and Ocean Research, Headland Sada, Vasco da Gama, Goa 403 804, India. (singhaaks@gmail.com)

2169-9380/13/10.1002/jgra.50488

Geomagnetic Effects chain in European region [*Kallio et al.*, 2000; *Tanskanen*, 2009] and AE_{TH} indices from Thermal Emission Imaging System chain over Canada and Alaska [*Angelopoulos et al.*, 2008] have been used for substorm studies. However, these local indices are relevant to the substorms only when the stations used for computation of the indices were located near the midnight.

[5] *Gjerloev et al.* [2010] carried out a collaborative study of worldwide geomagnetic data from over 100 SuperMAG observatories and computed generalized auroral electrojet indices for 3 years (1999 – 2001). Recently, *Newell and Gjerloev* [2011a] computed equivalent SuperMAG auroral electrojet (*SME*) indices (*SMU* and *SML*, respectively, equivalent to *AU* and *AL*) for over three decades using data from around 100 Northern Hemisphere observatories in magnetic latitude range 40° – 80°. Inclusion of a large number of observatories for the SuperMAG indices has clear advantage over the conventional *AE* indices. *Newell and Gjerloev* [2011a] compared around 1100 Polar Ultraviolet Imager (UVI) substorm onsets with those observed by the *SML* and *AL* indices in 1997–1998. The *SML* index identified about 50% more onsets (which were common in Polar UVI) than the conventional *AL* index. In addition, majority of substorm onsets were first determined by Polar UVI, subsequently after around 4 min (median value) by the *SML* index and at the last by the *AL* index after about 8 min (median value). Therefore, on an average, the *SML* index identified onset of substorms about 4 min earlier than the *AL* index [*Newell and Gjerloev*, 2011a].

[6] The *SME* indices have immediately drawn the attention of the community due to obvious advantage over the *AE* indices [e.g., *Newell and Gjerloev*, 2011b; *Connors*, 2012; *Bala and Reiff*, 2012; *Mitchell et al.*, 2013]. It would be desirable to examine whether inclusion of a large number of stations to the *SME* indices affects the UT and seasonal variations of the auroral electrojets activities. In this work, we carry out a comparative study between the *AE* and *SME* indices with an emphasis on the UT and seasonal variations. In section 2, details of the data used for this study have been presented. Section 3 describes the UT and seasonal variations of the *AE* and *SME* indices. In section 4, the UT and seasonal variations of negative bay onsets in the *AL* and *SML* indices have been described. The discussion and conclusion follow in section 5.

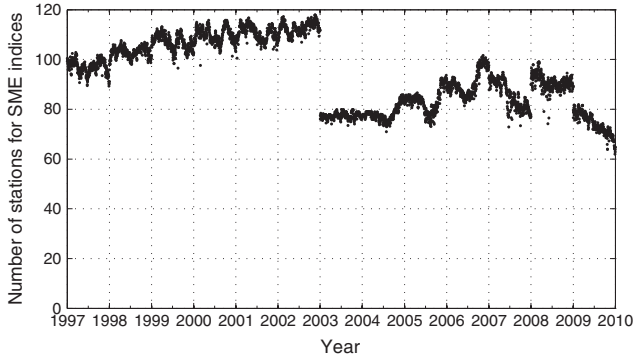

Figure 1. The number of stations available for the computation of *SME* indices during years 1997–2009.

2. Data

[7] For years 1997–2009, 1 min resolution *SME* indices and data of individual standard *AE* observatories were taken from the webpage of SuperMAG (http://supermag.jhuapl.edu/). For the computation of *SME* indices, data of individual stations were processed through automatic computer program (see *Gjerloev* [2012] for details). However, sometimes erroneous values may remain in the indices despite massive data processing. In our analysis, we removed exceptionally high *SME* values. It may be noted that the *SME* indices are not official International Association of Geomagnetism and Aeronomy indices due to the fact that SuperMAG is not restricted to specific set of stations for the computation of the indices, rather data of all the stations in latitude range 40° – 80° are included, when available to SuperMAG. Conventional *AE* indices of 1 min resolution were provided by World Data Center for Geomagnetism, Kyoto.

[8] Figure 1 shows the number of stations available for the computation of the *SME* indices for each of the days during years 1997–2009. The number of *SME* stations was consistently far more than those used for the *AE* indices. However, it may be noted that the number of *SME* stations is not constant over the selected period and a dramatic drop in the number of stations appears starting with year 2003.

3. UT and Seasonal Variations of the *AE* and *SME* Indices

[9] In this section, first we examine the UT and seasonal variations of the *AE* and *SME* indices which are, respectively, computed using around 12 and 100 stations data. However, it should be noted that the distribution of the *SME* stations is not uniform in local time. For example, a large number of stations are available over the American and European regions, whereas it is not the case everywhere. We took hourly averages of the *AU*, *AL*, *SMU*, and *SML* indices for each of the days of different months during years 1997–2009. As discussed by *Ahn et al.* [2000], simple averages at UT instances would be dominated by the quiet periods (quiet hours >> disturbed hours).

[10] Shown in Figures 2a and 2b are the UT and seasonal variations of the magnitudes of *AU* and *SMU* indices, respectively. The averaged *AU* and *SMU* values at each UT hour for a given month have been color coded. The *AU* and *SMU* indices maximize during local summer months (on *Y* axis) and attain lower values during winter. It clearly suggests that the eastward electrojet, which is believed as a directly driven component of the auroral electrojet activity, maximizes when the ionospheric conductivity is high due to the solar illumination in the summer months and minimizes when the ionospheric conductivity drops during the winter months [cf. *Ahn et al.*, 2000].

[11] There are important differences in the variations of the *AU* and *SMU* indices in UT (on *X* axis). Two prominent maxima are observed in the *AU* index (Figure 2a) separated by a minimum around 1500 UT. Although in Figure 2a, such UT pattern is clearly seen for summer months, when each month is plotted separately, the pattern remains consistent. *Ahn et al.* [2000] and *Lyatsky et al.* [2001] attributed

the prominent minimum to the unsuitable location of the *AE* stations in dusk hours (where eastward electrojet prevails) around 1500 UT. Mainly, stations Abisko (magnetic 65.5°N, 101.4°E) and Leirvogur (64.8°N, 66.5°E) would contribute to the *AU* index around 1500 UT. These stations often remain equatorward of the center of the eastward electrojet and hence the computed *AU* values remain quite low around 1500 UT. On the contrary, minimum around 1500 UT observed in the *AU* index, disappears in the *SMU* index for all months and broad maximum around 1000–2000 UT is observed (Figure 2b). It is possible that the inclusion of data from dense network of magnetic observatories over the American and European regions (in dusk hours when *SMU* maximizes) resulted in change in the UT variation of the *SMU* index. It should be noted that the level and range (represented by the color bars) of the *SMU* variations are consistently higher than those of the *AU* index. This could be primarily due to overall better representation of the eastward electrojet intensity by the *SMU* index in comparison to the *AU* index.

[12] Figures 2c and 2d depict the UT and seasonal variations of the magnitudes of the *AL* and *SML* indices, respectively. It is striking that both the indices exhibit grossly similar UT and seasonal variations despite the difference in the number of stations taken into account. In the winter solstice, two prominent minima during 0000–0700 UT and 2000–2300 UT are observed in the *AL* as well as *SML* and maxima in between (around 0800–2000 UT). It may be noted that the winter maximum in the *SML* appears relatively broader in UT hours and months than the *AL* maximum. During the summer solstice, occurrence of the *AL* maximum and minimum in UT hours are almost opposite to the UT pattern in winter season (Figure 2c). However, this fact is not as obvious in *SML* as for the *AL* index, particulary during 0500–1500 UT. Nevertheless, to some extent, relative similarities can be seen. As observed for the *AU* and *SMU*, the level and range of the *SML* variations are consistently higher than those of the *AL* index (see color bars in Figures 2c and 2d).

[13] The coexistence of the prominent minimum around 0000–0700 UT or 2000–2300 UT during winter months in the *AL* and *SML* indices shown in Figures 2c and 2d, cannot be attributed to the unavailability of stations [cf. *Ahn et al.*, 2000]. Several stations over Canada, Greenland, and Europe would be near midnight during these UT hours and hence significantly contribute to the *SML* index. The winter maximum in the *SML* index appears shifted towards early UT hours in comparison to the *AL* index, possibly due to excess stations over the Alaskan region.

3.1. Effect of the Solar Cycle on the UT and Seasonal Variations

[14] In order to examine the effect of the solar cycle on the UT and seasonal variations of the *AE* and *SME* indices, hourly indices of each day were binned into two groups based on the solar activity, (1) years 2000–2005 as high-sunspot years and (2) years 1997–1999 and 2006–2009 as low-sunspot years. Figures 3a and 3b, respectively, show the UT and seasonal variations of the *AU* and *SMU* indices for the high-sunspot years, whereas Figures 3c and 3d show the same for the *AU* and *SMU* indices, respectively, for the low-sunspot years. Color bars representing the magnitudes of the *AU* or *SMU* indices have been given on the right side of plots. As expected, the *AU* as well as *SMU* values are higher for active years when compared with those for the low-sunspot years (see scales on the color bars). The *AU* and *SMU* indices exhibit essentially similar UT and seasonal patterns as discussed in Figures 2a and 2b, respectively.

[15] The UT and seasonal variations of the magnitudes of the *AL* indices for high- and low-sunspot years are, respectively, shown in Figures 3e and 3g, whereas the same for *SML* indices for high- and low-sunspot years are shown in Figures 3f and 3h, respectively. Other than differences in magnitudes of indices for different solar activity phases, characteristics of the UT and seasonal variations of respective indices remain grossly similar. It, therefore, suggests that the UT and seasonal variations of the *AE* or *SME* indices are least sensitive to the phases of the solar cycle. Nevertheless, the overall geomagnetic activity responds significantly to the varying solar conditions.

[16] As mentioned above, the contour plots shown in Figures 2 and 3 would be dominated by magnetic quiet periods. In the next section, we examine the UT and seasonal variations of the number of negative bay onsets in the *AL* and *SML* indices as identified by *Newell and Gjerloev* [2011a] criteria. Since the westward electrojet, represented by *AL* or *SML* indices, is closely related to the substorm process [*Kamide and Rostoker*, 2004; *Newell and Gjerloev*, 2011a], 1 min resolution *AL* and *SML* indices have been used further.

4. Negative Bay Onsets in the *AL* and *SML* Indices

[17] For the identification of negative bay onsets in the *AL* and *SML* indices, we have used *Newell and Gjerloev* [2011a] algorithm. A sliding window of 30 min *SML* (and *AL*) data of 1 min resolution was examined. An onset time was identified at time t_o when the following four conditions were satisfied:

$$SML(t_o + 1) - SML(t_o) < -15 \text{ nT} \quad (1)$$

$$SML(t_o + 2) - SML(t_o) < -30 \text{ nT} \quad (2)$$

$$SML(t_o + 3) - SML(t_o) < -45 \text{ nT} \quad (3)$$

$$\sum_{i=4}^{i=29} SML(t_o + i)/26 - SML(t_o) < -100 \text{ nT} \quad (4)$$

Once an onset point t_o is identified, the algorithm advances ahead 20 min and selects another 30 min window. The above criteria insure steep and sustained depressions in the indices, which are typical of geomagnetic substorms. The same algorithm (equations (1)–(4)) was also applied to the *AL* index for identification of negative bay onsets in the *AL* index.

[18] It should be noted that in equation (4), values of i vary from 4 to 29 (26 points) instead of 4 to 30 (27 points) as in *Newell and Gjerloev* [2011a]. P. T. Newell (personal communication, 2013) confirmed the textual error in [*Newell and Gjerloev*, 2011a]. However, their programming code was the same as given above in equation (4). The list of substorm events available on the webpage of SuperMAG can be reproduced with the set of equations given above.

[19] The above mentioned criteria identified 24,288 negative bay onsets in the *SML* index, compared to 20,578 onsets

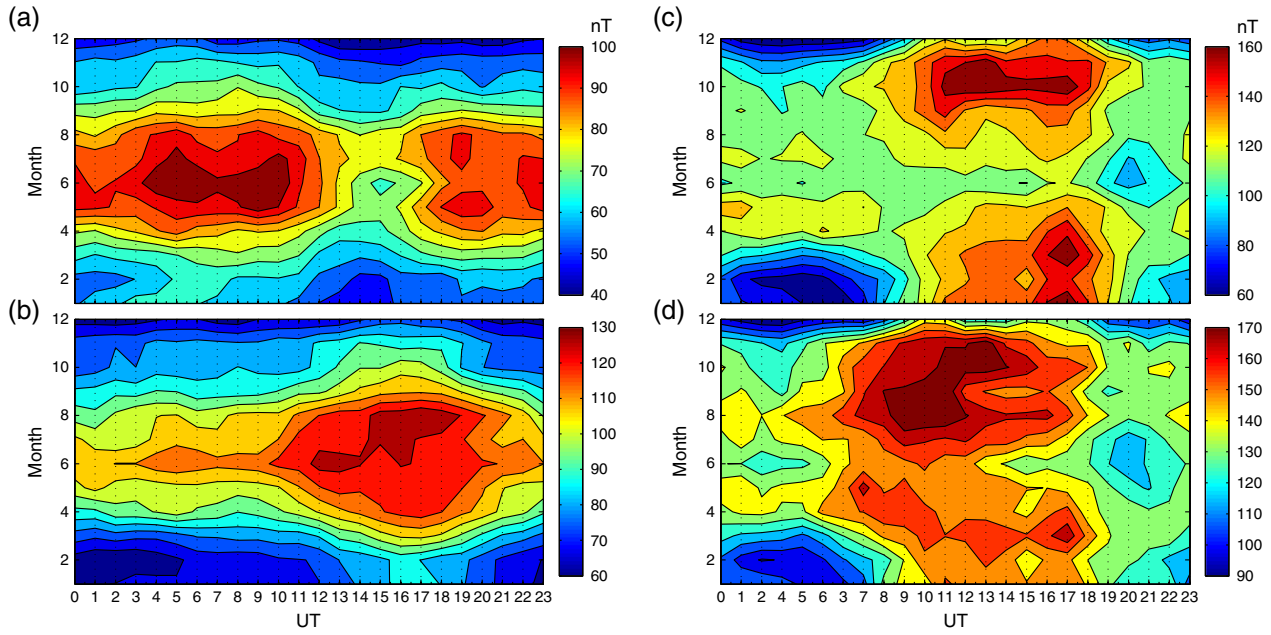

Figure 2. UT and seasonal variations of *AE* (*AU* and *AL*) and *SME* (*SMU* and *SML*) indices for years 1997–2009. (a) *AU* and (b) *SMU* indices show profound UT and seasonal variations. Both indices (*AU* and *SMU*) maximize during local summer month; however, there are subtle differences in the UT pattern. (c) Magnitude of *AL* and (d) magnitude of *SML* maximize during 0700–1800 UT in equinox and winter months. Moreover, prominent minimum is observed during 0000–0700 UT and 1900–2300 UT in winter.

in the *AL* index during years 1997–2009. The advantage of including a large number of stations for the *SML* index is clearly evident as around 18% more negative bay onsets were observed in the *SML* index than those in the *AL* index. It is important to note that the negative bay onsets selected by the algorithm could be produced by different processes, namely, the substorm current wedge (mainly in the midnight sector), the westward convection electrojets (in the dawn and dusk sectors at higher latitudes), and also poleward boundary intensifications (PBIs on the poleward branch of the oval). Therefore, all the identified negative bay onsets may not qualify the criteria for a legitimate substorm expansion phase onset [e.g., *Rostoker*, 2002]. Here, the term "onset" does not essentially represent the onset of a substorm expansion phase but rather represents initiation of a negative bay.

[20] Figure 4a depicts yearly distribution of negative bay onsets observed in the *SML* index (black bar) and *AL* index (gray bar). It is evident that the *SML* index consistently shows a larger number of onsets than those detected using the standard *AL* index. In Figure 1, it has been shown that the number of stations for *SME* indices suddenly drop at the start of year 2003. Nevertheless, the largest number of negative bay onsets was observed in the *SML* as well as *AL* indices for year 2003.

[21] The black curve in the figure shows yearly averaged sunspot number (multiplied by a constant factor 30 for the sake of visualization) for years 1997–2009. The number of onsets was clearly very high during the declining phase of solar cycle. It is well known that the high-speed solar wind streams originating from the coronal holes during declining phases of solar cycles result in a larger number of substorms [e.g., *Tanskanen et al.*, 2011, and references therein].

[22] Corrected geomagnetic (CGM) latitude and magnetic local time (MLT) of the stations contributing to the *SML* index at each minute (ideally one station at a time) are provided by SuperMAG. However, similar information is not available for the standard *AL* index. We extracted the CGM latitude and MLT of stations contributing at the time of onset of *SML* negative bays. Shown in Figures 4b and 4c (by squares) are, respectively, UT variations of the latitude and MLT of the contributing stations at the onsets. Although most of the onsets in Figure 4b were observed between 60° and 70° latitude, there were several onsets towards polar latitudes as well. In addition, at the time of onset of negative bays, mainly stations located on the night side of the Earth contributed to the *SML* variations (Figure 4c).

4.1. UT and Seasonal Variations of the Negative Bays

[23] The negative bay onsets identified in the *AL* and *SML* indices were binned in UT hours for each month and have been shown in Figures 5a and 5b, respectively. The average number of onsets within each UT hour for different months has been color coded. As observed in Figure 2c, here also, we see clear minima around 0000–0700 UT and 2000–2300 UT and a broad maximum around 0800–1900 UT in winter season for the *AL* onsets (Figures 5a). Occurrence of negative bays in the *AL* index are persistently lower in summer season, except for the weak indication of a maximum around 0000–0300 UT (Figure 5a). Grossly similar features are reflected for the *SML* negative bay onsets (Figure 5b). However, there is a certain difference in the *AL* and *SML* maxima during winter season. For the *SML* onsets, the maximum appears shifted towards early UT hours and also extends towards summer (Figure 5b).

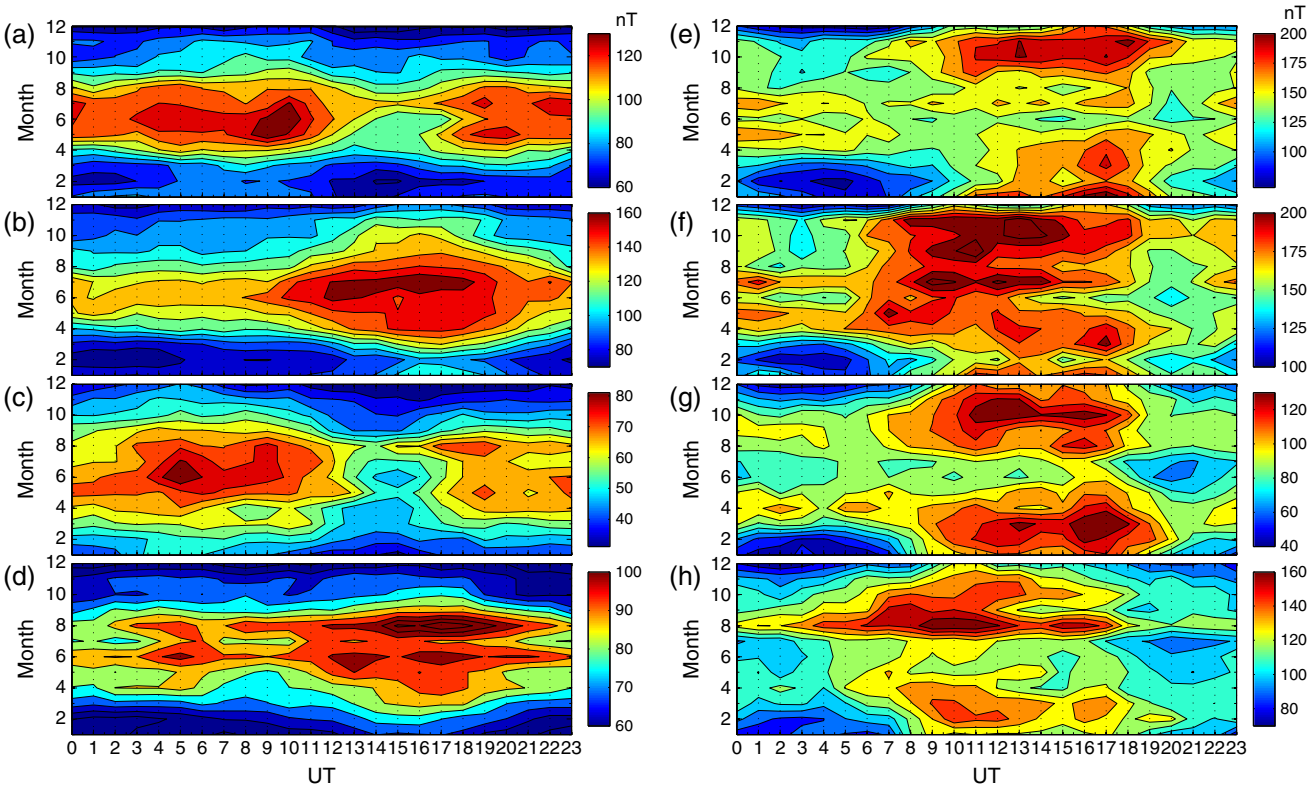

Figure 3. UT and seasonal variations of *AE* and *SME* indices for maximum and minimum phases of solar cycles. (a) UT and (b) seasonal variations of *AU* and *SMU* indices, respectively, for solar maximum years (2000–2005) and (c) UT and (d) seasonal variations of *AU* and *SMU* indices, respectively, for solar minimum years (1997–1999 and 2006–2009). (e, f) solar maximum years for *AL* and *SML* indices, respectively, and (g, h) same as Figures 3e and 3f but for solar minimum years.

4.2. Latitudinal and MLT Characteristics of the AL and SML Onsets

[24] As the *SME* indices include stations above 70° magnetic latitude as well, several negative bays in the *SML* index identified by the *Newell and Gjerloev* [2011a] algorithm could be associated with the poleward boundary intensifications (PBIs) or westward convection electrojets. *Rostoker* [2002] showed that PBIs are not only different in characteristics from the legitimate substorm onsets but also they initiate in the different region of the magnetotail. Moreover, westward convection electrojets are directly driven and remain localized towards the dawn or dusk sides at higher latitudes [*Kamide and Kokubun*, 1996].

[25] We divided the *SML* negative bays onsets into two groups: (1) above 70° magnetic latitude and (2) below 70° magnetic latitude. Hourly UT distribution of the *SML* onsets (or intensifications) above and below 70° magnetic latitudes have been shown in Figures 6a and 6b, respectively. As evident from the figure, onsets below 70° latitude are about 2 – 3 times higher when compared with those occurring above 70° latitude. Moreover, the UT variations of the two groups of onsets are quite different, particularly during 15–23 UT. The primary maximum for negative bays occurring above 70° latitude is observed during 15–18 UT (Figure 6a). On the contrary, a distinct minimum is observed in the same UT interval for onsets below 70° latitude (Figure 6b).

[26] During 15–18 UT, the Russian landmass would be in the magnetic midnight region. As most of the stations over Russia are equatorward of 70° magnetic latitude, it is very unlikely that the stations around the midnight would contribute to the primary maximum observed around 15–18 UT (in Figure 6a). In order to confirm this, we examine the MLT distribution of the *SML* negative bays observed poleward and equatorward of 70° latitude. Figure 6c clearly demonstrates that most of the negative bays above 70° latitude occurred around dawn hours in addition to significant contribution from pre-midnight sector. It is likely that the westward convection electrojets flowing towards the higher latitudes in the dawn and dusk meridians contribute to the maxima appearing in Figure 6c. Onsets below 70° are predominantly localized towards the midnight (see Figure 6d) in conformity with earlier studies [e.g., *Wang et al*., 2005].

[27] We further examined the UT and seasonal variations of the legitimate substorm expansion phase onsets which are believed to occur around MLT midnight and equatorward of 70° magnetic latitude [*Rostoker*, 2002]. We accordingly selected the *SML* negative bay onsets occurring below 70° magnetic latitude during 2100–0300 MLT. Since the MLT and latitude information at each minute for the *SME* indices were made available by SuperMAG, we could easily filter out legitimate substorms in the *SML* index by automatic program. However, for the identification of legitimate substorm

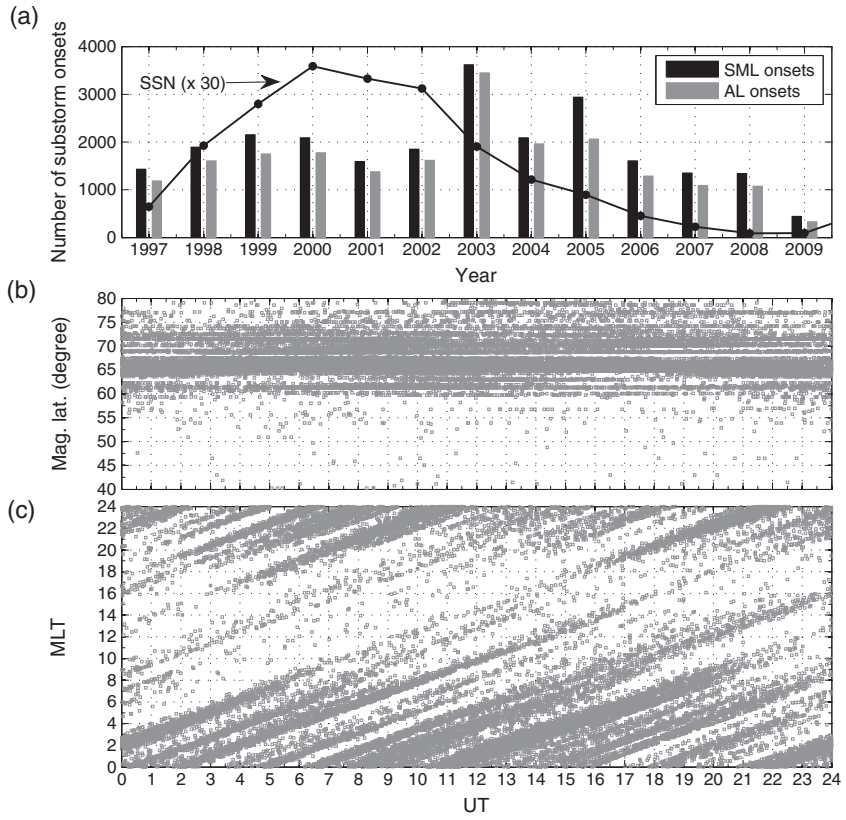

Figure 4. (a) Comparison of negative bay onsets in *SML* and *AL* indices (based on *Newell and Gjerloev* [2011a] algorithm) for years 1997–2009. *SML* index consistently identifies more number of onsets than those observed by *AL* index. Yearly averaged sunspot number (multiplied by 30 for the sake of representation in the same panel) has been shown by dotted black curve. (b) UT variations of magnetic latitude and (c) MLT of onsets as identified from *SML* index during years 1997–2009.

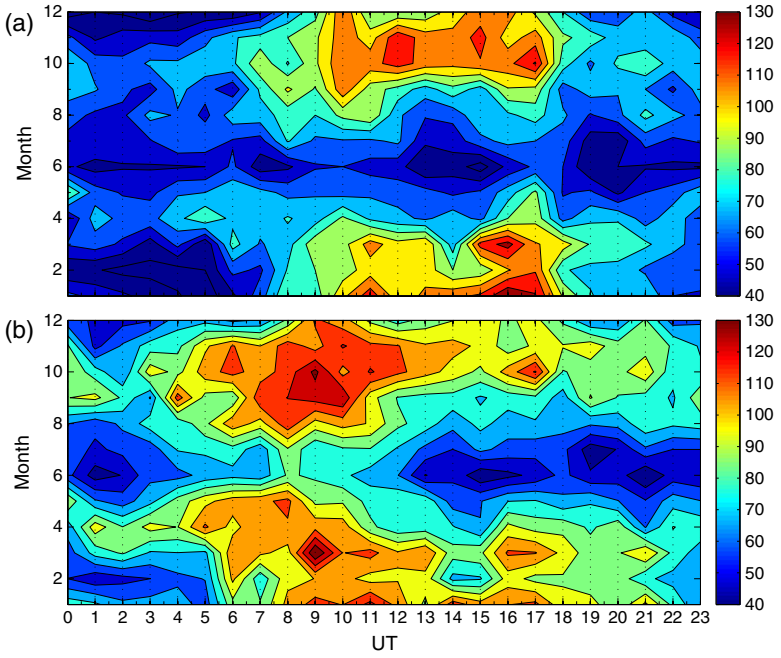

Figure 5. UT and seasonal variations of number of onsets identified from (a) *AL* index and (b) *SML* index for years 1997–2009. During local summer, a somewhat smaller number of onsets are observed at all UT hours while during equinox and winter seasons, very prominent UT preference of onsets are observed.

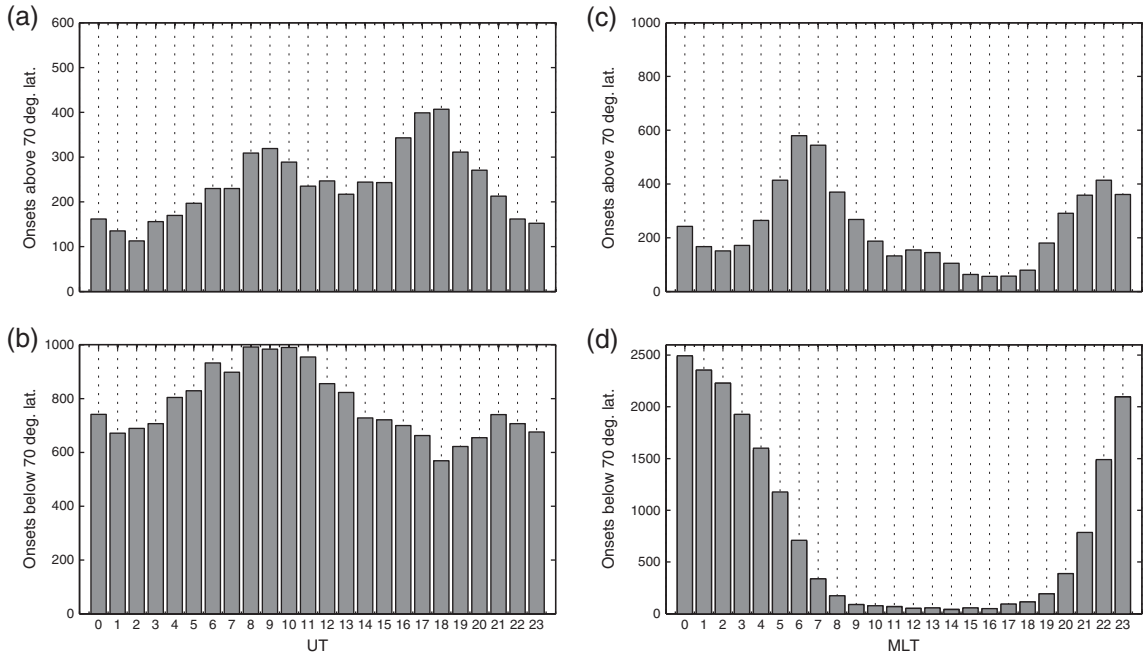

Figure 6. UT variations of *SML* onsets (a) above 70° latitude and (b) below 70° latitude. In addition to subtle differences in the UT patterns, onsets above 70° latitude are about 2–3 times less than those observed below 70° latitude. MLT distribution of *SML* onsets (c) above 70° latitude and (d) below 70° latitude.

onsets in the *AL* index, we recalculated *AL* index and retained the MLT of the contributing station by taking data of all available standard *AE* stations from SuperMAG for years 1997–2009. As all the standard *AE* stations (except Cape Chelyuskin) are located equatorward of 70° latitude, we considered each *AL* negative bay occurring during 2100–0300 MLT as a legitimate substorm.

[28] The UT and seasonal variations of the onset of legitimate substorms observed from the *AL* and *SML* indices have been shown in Figures 7a and 7b, respectively.

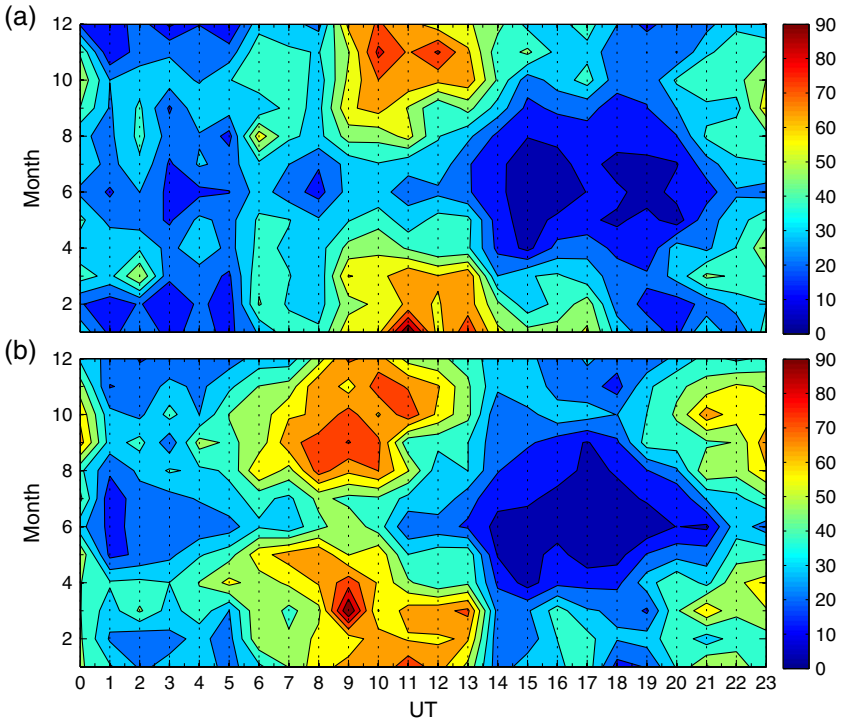

Figure 7. UT variations of (a) substorm onsets identified in *AL* during MLT midnight (2100–0300 MLT) and (b) substorm onsets in *SML* during MLT midnight (equatorward of 70° latitude).

The total number of substorm onsets at each UT hour for a given month has been color coded. Typical UT and seasonal characteristics of the *AL* and *SML* onsets as discussed above in Figures 5a and 5b, respectively, are evident in Figure 7 as well. In addition, for the legitimate substorms in the *AL* and *SML* indices, the UT and seasonal variations of substorm onsets are quite similar and the shift of *SML* maximum (in Figure 5b) towards early UT hours almost disappears.

5. Discussion and Conclusion

[29] *Newell and Gjerloev* [2011a] used around 100 SuperMAG stations data (in latitude range 40° – 80°) to compute equivalent auroral electrojet (*SME*) indices, whereas only 10–12 stations (mainly between 60° – 70° latitude range) are taken for calculating standard *AE* indices. Inclusion of various closely situated stations for the *SME* indices had clear advantages over the *AE* indices. The substorm onsets determined by the *SML* index (and simultaneously confirmed by the Polar UVI) were about 50% more in number and about 4 min earlier in time than those identified by the conventional *AL* index [*Newell and Gjerloev*, 2011a].

[30] In this study, we investigated the UT and seasonal variations of the standard *AE* indices and generalized *SME* indices. Simple averages of the *AE* and *SME* indices at each UT hour, as well as the onset of sharp negative bays in the *AL* and *SML* indices have been examined. The *AU* and *SMU* indices maximizes during local summer months. However, the prominent *AU* minimum around 1500 UT [see *Ahn et al*., 2000; *Lyatsky et al.*, 2001] disappears in the *SMU* index for all the months. Rather, a broad maximum around 1000–2000 UT is observed in the *SMU* index (Figure 2b) possibly due to the contribution from the American and European observatories to the *SMU* index. Fairly similar UT and seasonal variations of *AL* and *SML* indices (Figures 2c and 2d) rule out the possibility of sparse distribution of stations contributing to the prominent UT (and seasonal) variations; instead, our results support the hypothesis of *Lyatsky et al.* [2001], which suggests that the solar illumination of the auroral ionosphere is an important factor controlling the UT and seasonal variations of the westward auroral electrojet. However, some differences in *AL* and *SML* variations, e.g., shift of *SML* maximum towards early UT hours, could be due to the distribution of stations.

[31] The level of geomagnetic activity definitely is modulated by the solar cycle. Magnitudes of the *AE* and *SME* indices are observed to be higher during the high-sunspot years of the solar cycle than those observed during low-sunspot periods. Moreover, characteristics of the UT and seasonal variations of respective *AE* and *SME* indices remain grossly similar for low- and high-sunspot periods (Figure 3).

[32] *Newell and Gjerloev* [2011a] developed an algorithm to identify sharp depressions in *AL* and *SML* indices which are typical of geomagnetic substorms. In this study, we used the same algorithm to identify negative bay onsets in the *AL* and *SML* data for years 1997–2009. Over the selected duration, about 18% more number of negative bay onsets were observed from the *SML* index when compared with those observed from the *AL* index.

[33] The number of *AL* as well as *SML* onsets clearly varied over solar cycle. A relatively large number of onsets were observed during the declining phase of the solar cycle, which is in agreement with earlier studies [e.g., *Tanskanen et al.*, 2011]. The *SML* onsets were predominantly observed poleward of 60° latitude and on the nightside. The negative bay onsets in the *SML* index occurring poleward and equatorward of 70° latitude exhibit different UT and MLT patterns. It could be primarily due to the difference in the nature of physical processes occurring at different latitudes, e.g., legitimate substorms below 70° latitude and PBIs and convection bays at higher latitudes [*Rostoker*, 2002].

[34] There is considerable evidence that the magnetic substorms and related processes are suppressed in the sunlit or summer hemisphere [e.g., *Newell et al.*, 1996; *Wang and Lühr*, 2007; *Singh et al.*, 2012b]. The UT and seasonal variations of the *AL* and *SML* onsets (in Figure 5) show prominent reduction in the onsets during summer months in conformity with the previous evidence. The UT variations of *AL* and *SML* onsets in different seasons are fairly consistent with the reports of *Lyatsky et al.* [2001]. The nighttime (2100–0300 MLT) negative bay onsets in the *AL* index and nighttime negative bay onsets in the *SML* index below 70° magnetic latitude are very likely generated by substorm current wedge and hence can be considered as legitimate substorms. The UT and seasonal variations of these *AL* and *SML* substorm onsets, shown in Figure 7, exhibit UT pattern which is again consistent with the hypothesis of *Lyatsky et al.* [2001]. It clearly suggests that the UT and seasonal variations of the substorm activity, represented by the *AL* index, is not due to the sparse distribution of standard *AE* stations, rather primarily controlled by the solar illumination of the auroral ionosphere.

[35] **Acknowledgments.** Part of this work has been done at the ESSO-National Centre for Antarctic and Ocean Research, Goa, India and the Instituto Nacional de Pesquisas Espaciais, Sao Jose dos Campos, Sao Paulo, Brazil. R. R.'s work at INPE was supported by the Brazilian FAPESP (2012/12049-1). We sincerely thank J. W. Gjerloev and P. T. Newell for the SuperMAG auroral electrojet indices. The standard indices were taken from the World Data Center for Geomagnetism website (http://wdc.kugi.kyoto-u.ac.jp/index.html). We gratefully acknowledge the following SuperMAG collaborators for the ground magnetometer data: The S-RAMP Database, K. Yumoto and K. Shiokawa; the SPIDR database; Intermagnet; the institutes who maintain the IMAGE magnetometer array; AARI data, O. Troshichev; Danish Meteorological Institute, O. Rasmussen and J. Watermann; CARISMA, I. Mann; the MACCS program, W. J. Hughes and M. Engebretson, as well as the Geomagnetism Unit of the Geological Survey of Canada; GIMA, J. Olson; MEASURE, UCLA IGPP, and Florida Institute of Technology; USGS, J. J. Love; MAGIC, C. R. Clauer; SAMBA, E. Zesta; 210 Chain, K. Yumoto; SAMNET, F. Honary; IMAGE, A. Viljanen; the SuperMAG initiative, J. W. Gjerloev.

[36] Robert Lysak thanks Gordon Rostoker and Jesper Gjerloev for their assistance in evaluating this paper.

References

Ahn, B.-H., H. W. Kroehl, Y. Kamide, and E. A. Kihn (2000), Universal time variations of the auroral electrojet indices, *J. Geophys. Res.*, *105*(A1), 267–275, doi:10.1029/1999JA900364.

Angelopoulos, V., et al. (2008), Tail reconnection triggering substorm onset, *Science*, *321*, 931–935, doi:10.1126/science.1160495.

Bala, R., and P. Reiff (2012), Improvements in short-term forecasting of geomagnetic activity, *Adv. Space. Res.*, *10*, S06001, doi:10.1029/2012SW000779.

Basu, S. (1975), Universal time seasonal variations of auroral zone magnetic activity and VHF scintillations, *J. Geophys. Res.*, *80*, 4725–4728.

Berthelier, A. (1976), Influence of the polarity of the interplanetary magnetic field on the annual and the diurnal variations of magnetic activity, *J. Geophys. Res.*, *81*, 4546–4552.

Cliver, E. W., Y. Kamide, and A. G. Ling (2000), Mountains versus valleys: Semiannual variation of geomagntic activity, *J. Geophys. Res.*, *105*, 2413–2424.

Connors, M. (2012), Comment on "Substorm growth and expansion onset as observed with ideal ground-spacecraft THEMIS coverage" by V. Sergeev et al., *J. Geophys. Res.*, *117*, A02205, doi:10.1029/2011JA017254.

Davis, T. N., and M. Sugiura (1966), Auroral electrojet activity index *AE* and its universal time variations, *J. Geophys. Res.*, *71*, 785–801.

Gjerloev, J. W. (2012), The SuperMAG data processing technique, *J. Geophys. Res.*, *117*, A09213, doi:10.1029/2012JA017683.

Gjerloev, J. W., R. A. Hoffman, S. Ohtani, J. Weygand, and R. Barnes (2010), Response of the auroral electrojet indices to abrupt southward IMF turnings, *Ann. Geophys.*, *28*, 1167–1182, doi:10.5194/angeo-28-1167-2010.

Kallio, E. I., T. I. Pulkkinen, H. E. J. Koskinen, A. Viljanen, J. A. Slavin, and K. Ogilvie (2000), Loading-unloading processes in the nightside ionosphere, *Geophys. Res. Lett.*, *27*(11), 1627–1630, doi:10.1029/1999GL003694.

Kamide, Y., and S.-I. Akasofu (1983), Notes on the auroral electrojet indices, *Rev. Geophys.*, *21*(7), 1647–1656, doi:10.1029/RG021i007p01647.

Kamide, Y., and S. Kokubun (1996), Two-component auroral electrojet: Importance for substorm studies, *J. Geophys. Res.*, *101*, 13,027–13,045, doi:10.1029/96JA00142.

Kamide, Y., and G. Rostoker (2004), What is the physical meaning of AE index? *EOS Trans. AGU*, *85*, 188–192.

Kamide, Y., et al. (1998), Current understanding of magnetic storms: Storm-substorm relationships, *J. Geophys. Res.*, *103*(A8), 17,705–17,728, doi:10.1029/98JA01426.

Lyatsky, W., P. T. Newell, and A. Hamza (2001), Solar illumination as cause of the equinoctial preference for geomagnetic activity, *Geophys. Res. Lett.*, *28*, 2353–2356.

Newell, P. T., C.-I. Meng, and K. M. Lyons (1996), Supression of discrete aurorae by sunlight, *Nature*, *381*, 766–767.

Newell, P. T., and J. W. Gjerloev (2011a), Evaluation of SuperMAG auroral electrojet indices as indicators of substorms and auroral power, *J. Geophys. Res.*, *116*, A12211, doi:10.1029/2011JA016779.

Newell, P. T., and J. W. Gjerloev (2011b), Substorm and magnetosphere characteristic scales inferred from the SuperMAG auroral electrojet indices, *J. Geophys. Res.*, *116*, A12232, doi:10.1029/2011JA016936.

Mitchell, E. J., P. T. Newell, J. W. Gjerloev, and K. Liou (2013), OVATION-SM: A model of auroral precipitation based on SuperMAG generalized auroral electrojet and substorm onset times, *J. Geophys. Res. Space Physics*, *118*, 3747–3759, (in press), doi:10.1002/jgra.50343.

Russell, C. T., and R. L. McPherron (1973), Semiannual variation of geomagnetic activity, *J. Geophys. Res.*, *78*, 92–108.

Rostoker, G. (1972), Goemagnetic indices, *Rev. Geophys.*, *10*, 935–950.

Rostoker, G. (2002), Identification of substorm expansive phase onsets, *J. Geophys. Res.*, *107*(A7), doi:10.1029/2001JA003504.

Singh, A. K., A. K. Sinha, R. Rajaram, and B. M. Pathan (2012a), Storm-time longitudinally propagating asymmetric modes at low latitudes, *Ann. Geophys.*, *30*, 131–141, doi:10.5194/angeo-30-131-2012.

Singh, A. K., A. K. Sinha, R. Rawat, B. Jayashree, B. M. Pathan, and A. Dhar (2012b), A broad climatology of very high latitude substorms, *Adv. Space Res*, *50*, 1512–1523, doi:10.1016/j.asr.2012.07.034.

Tanskanen, E. I. (2009), A comprehensive high-throughput analysis of substorms observed by IMAGE magnetometer network: Years 1993–2003 examined, *J. Geophys. Res.*, *114*, A05204, doi:10.1029/2008JA013682.

Tanskanen, E., T. I. Pulkkinen, A. Viljanen, K. Mursula, N. Partamies, and J. A. Slavin (2011), From space weather toward space climate time scales: Substorm analysis from 1993 to 2008, *J. Geophys. Res.*, *116*, A00I34, doi:10.1029/2010JA015788.

Vassiliadis, D., A. J. Klimas, D. N. Baker, and D. A. Roberts (1995), A description of the solar wind-magnetosphere coupling based on nonlinear filters, *J. Geophys. Res.*, *100*(A3), 3495–3512, doi:10.1029/94JA02725.

Wang, H., and H. Lühr (2007), Seasonal-longitudinal variation of substorm occurrence frequency: Evidence for ionospheric control, *Geophys. Res. Lett.*, *34*, L07104, doi:10.1029/2007GL029423.

Wang, H., H. Lühr, S. Y. Ma, and P. Ritter (2005), Statistical study of the substorm onset: Its dependence on solar wind parameters and solar illumination, *Ann. Geophys.*, *23*, 2069–2079.

Zhou, X.-Y., W. Sun, A. J. Ridley, and S. B. Mende (2011), Joule heating associated with auroral electrojets during magnetospheric substorms, *J. Geophys. Res.*, *116*, A00I28, doi:10.1029/2010JA015804.